Magnetoresistance of Co/Cu superlattices grown by molecular beam epitaxy

M. J. Hall, B. J. Hickey, M. A. Howson, M. J. Walker, J. Xu, D. Greig, and N. Wiser*
Department of Physics, University of Leeds, Leeds LS2 9JT, United Kingdom
(Received 25 August 1992; revised manuscript received 10 December 1992)

The giant magnetoresistance (GMR) has been investigated for Co/Cu superlattices grown by molecular beam epitaxy (MBE) with the copper and cobalt (111) planes parallel to the surface. When Au was used as a buffer layer, values of the GMR were found as high as 30%. Oscillations were observed in the saturation magnetic field as a function of the thickness of the Cu layer, but these oscillations were not observed in the GMR. The central purpose of the investigation was to study the effect on the GMR of annealing the superlattices and to interpret the changes in terms of the relative contributions to the resistivity of bulk and interface electron scattering. It was found that the magnitude of the GMR for the Co/Cu system decreases on annealing in sharp contrast to previous observations in Fe/Cr superlattices for which several workers have shown that the effect of annealing was normally to increase the GMR. This striking difference between the two systems is explained in terms of their very different spin dependence for interface electron scattering. A calculation is presented which accounts quantitatively for both our results for the Co/Cu system, and for the contrasting results in Fe/Cr.

I. INTRODUCTION

During the past few years, magnetic superlattices and multilayers have been the subject of intense experimental[1–34] and theoretical[35–48] investigations. Of particular interest for these materials is the fact that for certain specific thicknesses of the nonmagnetic spacer layer, neighboring magnetic layers are coupled antiferromagnetically and the system exhibits a giant magnetoresistance (GMR) of order 10–100 %. It is generally agreed that these two phenomena are related, although even for the two most widely studied systems, Co/Cu and Fe/Cr, much remains unclear.

For example, for the Co/Cu system, polycrystalline multilayers prepared by sputtering readily yield[18] a GMR as large as 100%. By contrast, unless special techniques are used, single-crystal superlattices grown by molecular beam epitaxy (MBE) very often fail to yield a GMR at all. Indeed, we reported[27] the first observation of a true GMR (of magnitude 26%) for an MBE-grown Co/Cu superlattice only very recently, using the "trick" of incorporating a thin gold layer as the final layer in the buffer region on top of the substrate. Another puzzling feature of the GMR relates to the change in its magnitude when the sample is annealed. For the Co/Cu system, annealing was found to decrease the GMR,[32] whereas for the Fe/Cr system the reverse is true, with annealing increasing the magnitude of the GMR.[12,31]

In two recent short papers[27,32] we reported some preliminary data for the GMR of an MBE grown Co/Cu superlattice, and its change in magnitude on annealing. In this paper, we shall present our results in detail, including magnetization measurements that indicate antiferromagnetic coupling for our superlattices. We also derive an expression that accounts quantitatively for the GMR data for annealed samples, both for the Co/Cu system that we have studied as well as for the Fe/Cr system studied by other workers.

II. EXPERIMENTAL RESULTS

The superlattices were grown in a VG 80M MBE facility on GaAs (110) substrates. The substrates were heated to about 600 °C until reflection high-energy electron diffraction (RHEED) indicates surface reconstruction characteristic of GaAs(110). It has been found[4] that depositing a 500-Å layer of Ge at 500 °C greatly improves the quality of the metallic layers. A single layer of bcc (110) Co is necessary to seed epitaxy, and is grown on the Ge at a temperature of about 150 °C. Having experimented with both Cu [200 Å, (111)] and Au [10 Å, (111)] buffer layers, we found that only the Au buffers resulted in layers of sufficient quality to yield a giant magnetoresistance. We then grew 20 bilayers of nominally 15 Å of Co and thicknesses of Cu ranging from 5 to 22 Å.

The samples were characterized *in situ* by RHEED and *ex situ* by x-ray diffraction and x-ray pole figures. In Fig. 1, we show two orientations of the copper layers during growth. The patterns, separated by an angle of 30°, both show the streaky appearance that is the signature of flat surfaces, and both show the sixfold rotational symmetry that is a characteristic of the close-packed atomic arrangement in (111) growth. The surface of a (111) plane can be represented by a two-dimensional hexagonal net, and the labels in Fig. 1 represent the rows of atoms giving rise to the particular diffraction streak. For a hexagonal net, the lattice constant a is related to the separation d_{hk} of the rows (hk) by

$$d_{hk}^2 = (\tfrac{3}{4})a^2/(h^2+k^2+hk) ,$$

so that for the rows in question $d_{11}/d_{21}=\sqrt{3}$. As in any diffraction experiment, the separation of the lines or spots in the pattern is inversely proportional to the separation of the diffracting elements. We note that the excellent agreement between this value of $\sqrt{3}$ and the inverse ratio of the separations of the two set of RHEED streaks

shown in Fig. 1 provides further evidence that the growth planes parallel to the surface are (111).

Low-angle x-ray-diffraction peaks were visible at angles corresponding to the bilayer thickness and, for some samples, a second-order peak was visible indicating sharp interfaces. It is very difficult to see more than two low-angle Bragg peaks in Co/Cu, because the form factors for Co and Cu are so similar that there is a lack of x-ray contrast. It was found that the Cu was highly oriented in the [111] direction, with no sign of other orientations. For example, the ratio of intensities in the pole figures for the (111) and (110) planes was 500:1, which is within the signal-to-noise-ratio. Further details of the x-ray measurements can be found in Refs. 27 and 32.

Samples were cleaved into rectangular shapes such that the long side was in the $[\bar{1}12]$ GaAs direction. This does not correspond exactly to a crystal axis in the superlattice, but is 7° from the $[\bar{1}01]$ direction. The magnetoresistance was measured using a standard four-probe dc method, with pressure contacts in a longitudinal arrangement (current and field parallel). Samples for annealing were prepared by cleaving a large section into several smaller pieces.

Figure 2 shows the magnetoresistance at 5 K in fields up to 70 kOe. The data for the sample for which the copper thickness is 7 Å show a large change in resistance (30%) which is associated with antiferromagnetic (AFM) coupling, whereas the much smaller change (3%) for the 5-Å sample indicates that the coupling is predominantly ferromagnetic (FM). However, we emphasize that in all our samples the field required for saturation of the magnetoresistance is very large, which indicates very strong exchange coupling between the magnetic layers.

Figure 3 shows the effect of changing the current-field orientation from parallel to transverse for a sample of composition $[Co(12\ Å)Cu(9\ Å)]_{20}$ for which the GMR is over 30%. Although we reported previously[27] that changing the geometry had no effect on the magnitude of the magnetoresistance, this earlier result was for fields of less than 8 kOe, and this absence of field dependence at low fields is confirmed in Fig. 3. However, above 8 kOe there is a small difference between the longitudinal and transverse magnetoresistance. The field dependence of this difference tells us something about the magnetization process. At saturation, this difference is simply due to the anisotropic magnetoresistance,[49] which has a value of about 2%. On the other hand, the fact that there is no difference between the two geometries up to about 8 kOe implies that the magnetization direction is not affected by the external field. A difference then begins to appear as

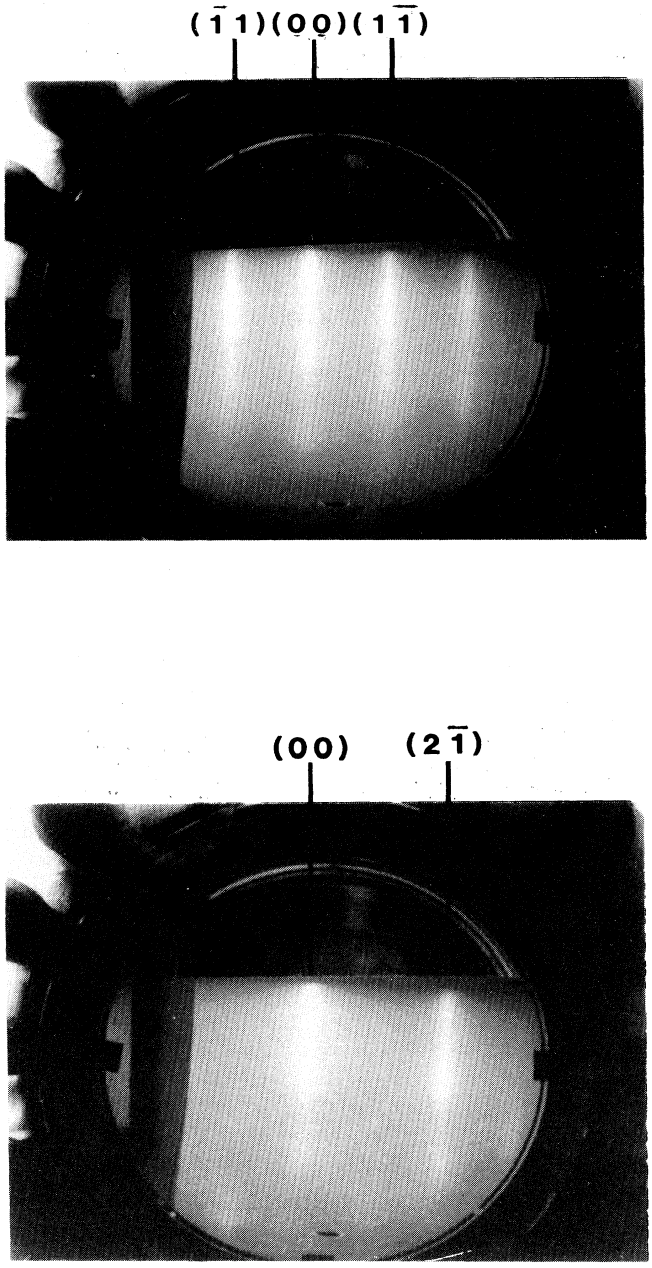

FIG. 1. RHEED patterns on two orientations of the copper surface during growth. The indices refer to the hexagonal net on the (111) surface.

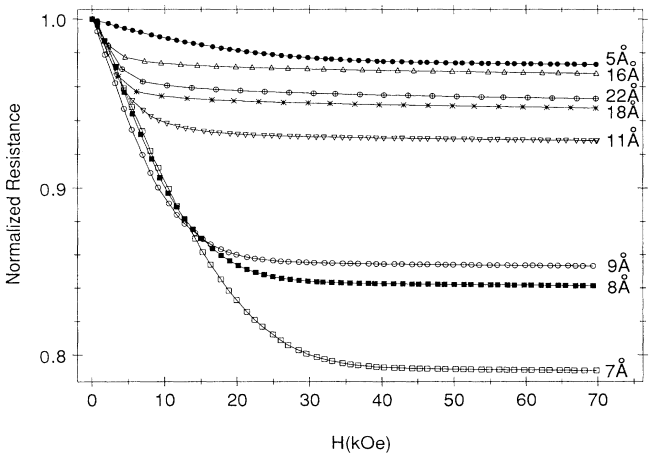

FIG. 2. The field dependence of the normalized resistance of Co/Cu superlattices with various copper thicknesses.

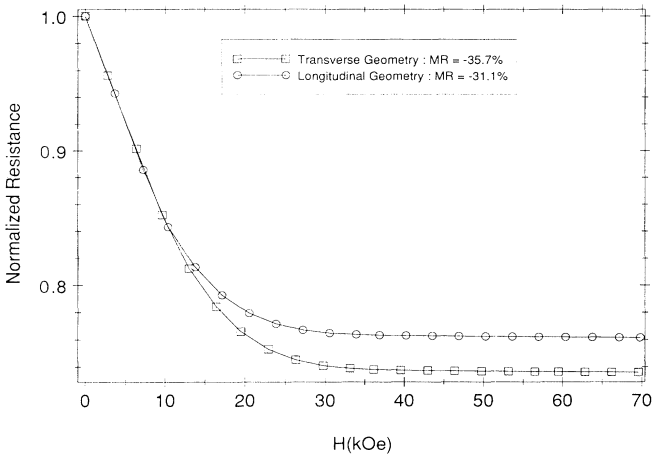

FIG. 3. The field dependence of the normalized resistance for a sample with a copper spacer of 7 Å, measured in both the longitudinal and transverse configurations.

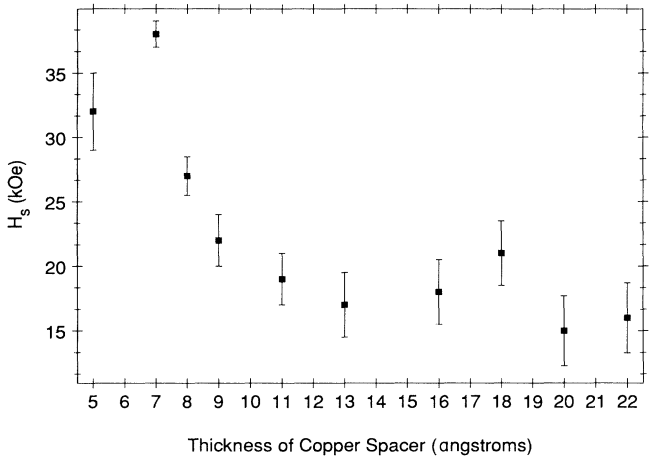

FIG. 5. The saturation magnetic field vs the copper spacer thickness.

the magnetization in each layer rotates toward the direction of the field.

In Fig. 4, we show some first measurements of the magnetization of these materials in samples for which the thicknesses of the copper layers are 5 and 7 Å. There is a clear difference in the two magnetization curves. The 5-Å sample has a large remnant magnetization but small saturation field, whereas the 7-Å sample has a much smaller remnant magnetization and a large saturation field. The saturation field for the 7-Å sample is about 40 kOe, which is consistent with the saturation of the magnetoresistance. These values of saturation field and remnant magnetization are typical of an AFM-coupled superlattice and are similar to the values found in sputtered Co/Cu multilayers.[7] By contrast, the large remnant magnetization of the 5-Å sample is consistent with predominantly FM coupling. Although the saturation field is smaller in the 5-Å sample, it is still larger than expected for simple FM coupling, and may suggest either a mixture of AFM and FM coupling or the presence of in-plane anisotropy.

In Fig. 5, we show the variation of saturation fields determined *from the GMR* as a function of copper layer thickness, from which one can see oscillations with peaks in the saturation fields at 7 and 18 Å. The criterion for determining the saturation field was to extrapolate the high-field background to lower fields and estimate where the GMR deviated from this background. Although the uncertainties in this process are quite large, as indicated by the error bars, the evidence for the second peak at 18 Å is quite apparent. However, in Fig. 6, where we show the percentage change of the magnetoresistance at saturation fields as a function of Cu thickness, the evidence for a second peak in the GMR itself is not so clear. Nevertheless we emphasize that it is not necessary for the GMR to exhibit the same oscillations as the saturation

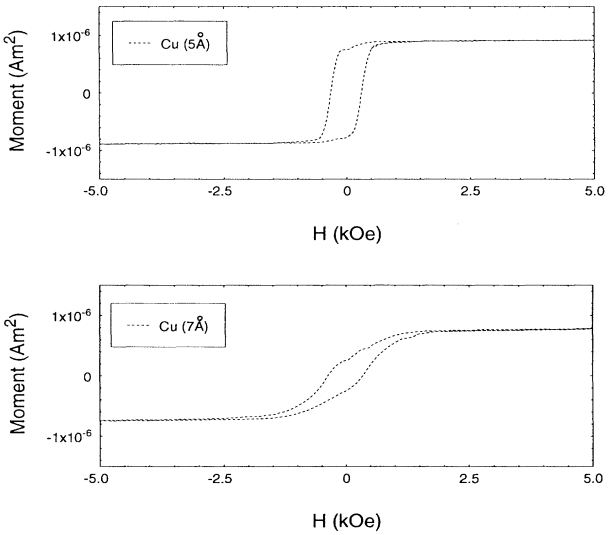

FIG. 4. The magnetization of the superlattices with 5- and 7-Å copper spacer layers.

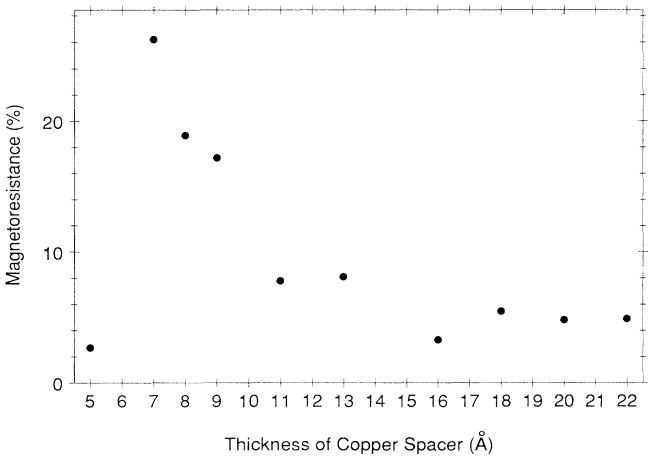

FIG. 6. The saturation value of the magnetoresistance vs the copper spacer thickness. The uncertainties are smaller than the size of the points.

field, as this depends only on the strength of the coupling, whereas the GMR also depends on other factors such as the ratio of bulk to interface scattering.

It is worth highlighting the differences between our results for MBE-grown samples and previous results on samples prepared by sputtering. For the latter, it has been found that the saturation fields are small (< 10 kOe), so the AFM coupling is relatively weak, but in our MBE samples the AFM saturation fields are large (≈ 40 kOe), and the coupling strong. In the sputtered films, there are oscillations as a function of Cu thickness with a period of about 10 Å in both the saturation field and the GMR, whereas in our MBE-grown samples there are oscillations of a similar period only in the saturation field, with only one maximum in the value of the GMR. We believe that the difference in the dependence of the GMR on the Cu thickness could be correlated with the difference in the ratio of the bulk to interface scattering, and herein lies a major difference between the sputtered and MBE-grown samples. In sputtered samples, which are textured polycrystalline films, we may assume that although the interface scattering can be strong, the scattering is, nevertheless, dominated by bulk scattering. In MBE samples, which are epitaxially grown with a high degree of crystallinity, bulk scattering is much reduced.

Although we noted that the magnitude of the saturation magnetic field is comparable for the GMR and for the magnetization, the actual field dependence of these two quantities is very different. Comparing the magnetoresistance of the sample with 7-Å copper layers (Fig. 2) with the magnetization data (Fig. 4), we note that the magnetic field needed to produce significant changes in the electrical resistance is considerably greater than the field required to produce a significant degree of magnetization. This striking difference can be explained in terms of the competition between the AFM exchange coupling and the in-plane anisotropy.

In Fig. 7, we show the low-field magnetoresistance data at room temperature for the 7-Å sample on an expanded scale up to a maximum field of 800 Oe. The most interesting feature is a marked coercive field of approximately 50 Oe showing that, even though the large saturation field indicates AFM coupling, there is also some degree of FM alignment. This highlights the importance of looking at both low-field and high-field magnetization measurements, as the low-field data may indicate FM coupling even though the coupling is predominantly AFM.

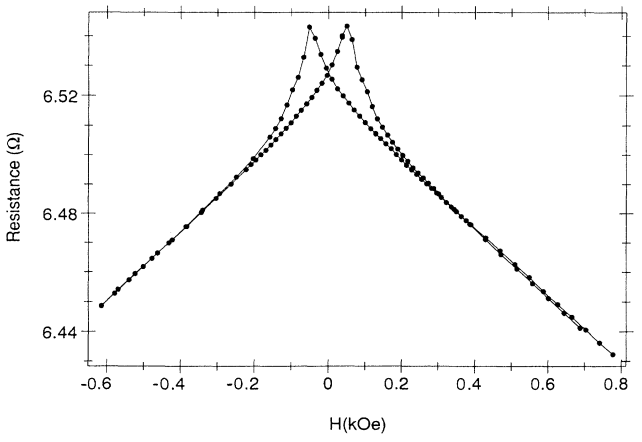

FIG. 7. The field dependence of resistance for a sample with a copper space of 7 Å in the low-field regime.

III. EFFECT OF ANNEALING ON THE GMR

There is currently an unresolved question regarding the dominant electron-scattering process that gives rise to the GMR. The analysis of the GMR by Edwards, Mathon, and co-workers[41–45] was based on the spin-dependent scattering of electrons in the bulk of the magnetic layers, whereas Levy, Zhang, and co-workers[37–40] have emphasized the importance of spin-dependent electron scattering at the interfaces between the magnetic and the nonmagnetic layers. Our experiments were designed to change the interface roughness by annealing the superlattice and thus shed light on this controversy by analyzing the observed changes in the measured GMR in terms of the relative contributions of interface and bulk electron scattering.

Previous workers[12,23–25,31] who carried out similar measurements on the Fe/Cr system found that, regardless of whether the multilayers were produced by sputtering or by MBE, and regardless of whether the interfacial roughening was caused by annealing or by changing the pressure of the sputtering gas, "increasing roughness always resulted in enhanced magnetoresistance."[25] In complete contrast to these results for the Fe/Cr system, our measurements on Co/Cu multilayers yield a progressive decrease in the value of the MR on annealing. Moreover, we shall show that the different results obtained for the two systems can both be explained in terms of the increase of interface electron scattering caused by annealing.

A. Co/Cu superlattices

Our low-temperature data for the change in the GMR on annealing a Co/Cu superlattice are displayed in Fig. 8, where the magnetoresistance is plotted as a function of the zero-field resistivity ρ_0 of the sample. The open circle represents the data point for the unannealed sample, whereas the full symbols give the results for the annealed samples. Annealing causes an overall increase in electron scattering which increases ρ_0. It can be seen that successive annealing of the Co/Cu superlattice leads to a progressive reduction of the MR. The curves in Fig. 8 represent an analytical fit to the data which we shall discuss in a later section.

We note in Fig. 8 that, depending on the temperature range under consideration, the annealing treatment took several different forms. (a) At the lowest temperatures, different pieces cut from the same unannealed Co/Cu superlattice were annealed for 1 h at temperatures between 230 and 275 °C. (b) At slightly higher temperatures in the narrow range between 280 and 295 °C, annealing the 275 °C sample for only 10 min at progressively higher temperatures leads to a marked decrease in the MR with

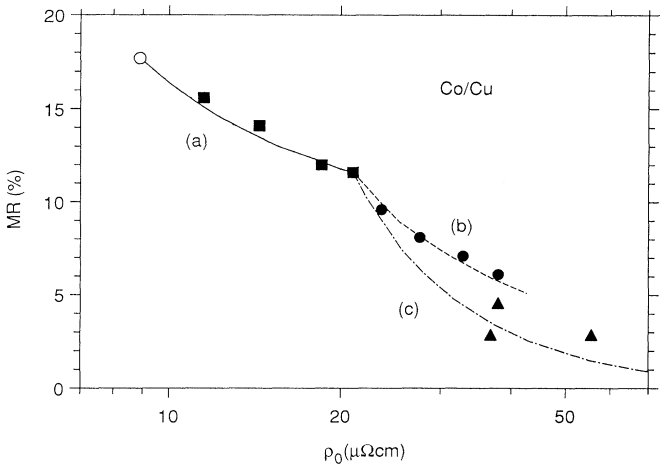

FIG. 8. The saturation magnetoresistance vs the zero-field resistivity for Co/Cu superlattices annealed at various temperatures. The symbols are explained in the text, and the lines are theoretical fits discussed in the text.

increasing ρ_0. (c) Finally, samples were annealed at 300 °C for varying periods of time (10 min, 30 min, and 1 h), and this yielded a still greater decrease in the MR and a complete loss of low-angle peaks in the x-ray scans. The data points corresponding to the three forms of annealing are depicted in Fig. 8 by squares, circles, and triangles, respectively.

These experimental results can be understood in the following way. It is generally agreed that the GMR observed in magnetic superlattices and multilayers results from the antiferromagnetic coupling between neighboring magnetic layers. In the antiferromagnetic configuration, electron scattering is on average independent of its spin direction as the electron travels through successive layers. Applying a saturation magnetic field to align the superlattice into the ferromagnetic configuration then leads to a strong dependence of electron scattering on spin direction (assuming no spin mixing, as is appropriate at low temperatures). It is easy to show[44] that such a system exhibits a GMR whose magnitude depends on the ratio of the scattering probability of the spin-up electrons to that of the spin-down electrons.

A theoretical analysis of the GMR in terms of a "resistor network" model has been given by Edwards, Mathon, and Muniz,[42] who emphasized bulk scattering of the electrons in the magnetic host. Based on the marked spin dependence of the d-band density of states at the Fermi energy of the magnetic layers, Edwards, Mathon, and coworkers[42–45] have calculated the GMR, obtaining a magnitude for the Co/Cu system that is in good agreement with the largest measured values as a function of layer thickness.

Now consider the scattering of an electron at the interfaces between the Co and the Cu layers of the superlattice. Electron scattering at the Co/Cu interface is "catastrophic," in that the electron loses all memory of its momentum when diffusely scattered. Therefore the scattering is independent of the bulk density of states and hence independent of the direction of the electron spin which serves to reduce the magnetoresistance. The more spin independent the scattering, the smaller the value of the MR. Because annealing the Co/Cu superlattice increases interface scattering, it follows that annealing should decrease the MR. This is indeed what we observe for Co/Cu superlattices.

We have made these ideas quantitative by including interface scattering in the "resistor network" model[42] by adding additional "resistors" into the network for each spin direction to represent interface scattering. The details of the calculation will be described in the next section, and here we give the principal result:

$$\mathrm{MR}=\frac{[\frac{1}{2}p_b(\alpha_b-1)+p_i(1+r)(\alpha_i-1)]^2}{[p_b(\alpha_b+r)+2p_i(1+r)(1+\alpha_i)][(p_b+4p_i)(1+r)]}\ , \tag{1}$$

where r is the ratio of the thicknesses of the Cu and the Co layers, and p_b and p_i represent the proportion of the electron scattering that takes place in the bulk (subscript b) and at the interfaces (subscript i), respectively, where $p_b+p_i=1$. The value of p_b for the unannealed superlattice is chosen to make the calculated value of MR equal the measured MR for that sample.

The key quantities in (1) are α_b and α_i which denote, respectively, the ratio of spin-down electron scattering to spin-up electron scattering in the bulk (b) of the magnetic layers and at the interfaces (i). For the Co/Cu system, Edwards and co-workers[42–45] find that in the absence of interface scattering, the value $\alpha_b=8$ accurately reflects the strong spin dependence of the bulk density of states in ferromagnetic Co. Since, for Co/Cu, interface scattering is independent of the direction of the electron spin, $\alpha_i=1$.

The four squares in Fig. 8 corresponding to $\rho_0<21$ $\mu\Omega$ cm refer to Co/Cu superlattices for which the annealing temperature has been kept below 280 °C. At such low annealing temperatures, the structural integrity of the interface is maintained, as has been confirmed by x-ray scans.[32] The effect of annealing is to cause diffusion of the Cu atoms into the neighboring Co layers and vice versa. Part of this diffusion is restricted to the interface and part penetrates into the bulk. However, this distinction is not clearcut. From Eq. (1), the change in magnetoresistance due to annealing is due to the change in the relative fraction of bulk (p_b) and interface (p_i) scattering. The change in the ratio (p_b/p_i) is used as a fitting parameter, and is related to the net resistivity of the superlattice by Eq. (11) below. We find the best overall fit to the data

by assuming that about half the additional scattering due to annealing arises from interface scattering ($p_i = 57\%$) and about half arises from bulk scattering ($p_b = 43\%$). This leads to the calculation curve (a)—the full curve in Fig. 8—which shows excellent agreement with experiment.

It should be noted that the reduction of the magnetization of the Co layers due to the diffusion of Co atoms into the Cu layers is negligible. The measured increase in resistivity on gentle annealing up to 275 °C is about 12 $\mu\Omega$ cm, which would result from the additional impurity scattering due to about 2% Co in Cu.[50] Since, for our samples, the cobalt layers are about twice as thick as the copper layers, the decrease in thickness of the Co layers cannot be greater than 1%, and the overall magnetic structure of the superlattice is virtually unchanged.

We now consider the somewhat higher annealing temperatures in the range 280°–295°. Annealing at these temperatures begins to undermine the structural integrity of the interface and yields the data points given by the four circles in Fig. 8. As a result, a greater proportion of the electron scattering takes place at the interface, which should lead to a more rapid decrease in MR with ρ_0. Such behavior is clearly evident in the data.

Analytically we take this incipient structural breakdown into account by assuming in Eq. (1) that a greater proportion (80%) of the additional scattering due to annealing arises from interface scattering. This yields the calculated curve (b)—the dashed curve in Fig. 8—and again the data points (the circles) are seen to be in agreement.

Finally, we consider the data points obtained by annealing the superlattice at 300 °C. At such a high annealing temperature, the x-ray scans[32] indicate an almost complete breakdown of the interfacial integrity. Consequently, the decrease in MR with increasing ρ_0 should be even more rapid, and this is indeed found to be the case. Theoretically, this structural breakdown is taken into account by assuming in Eq. (1) that *all* the additional electron scattering due to annealing arises from interface scattering. This yields the calculated curve (c)—the dot–dash curve in Fig. 8—and once again the data points (the triangles) are in satisfactory agreement with the calculation.

B. Fe/Cr superlattices

We suggest that the reason why the Fe/Cr system is so different is because of a phenomenon that does not occur for Co/Cu superlattices. This is the strong spin dependence of electron scattering of Cr impurities in an Fe host,[51,52] which results in spin-dependent scattering at the interfaces. Friedel[53] has shown that this spin dependence arises from the resonant scattering of the virtual bound state of a Cr atom in the *d* band of ferromagnetic Fe. This spin-dependent interface scattering formed the basis for the successful calculation of the GMR for Fe/Cr superlattices carried out by Levy, Zhang, and coworkers.[37–40] We argue that this same resonant scattering—which is entirely absent in the Co/Cu system—is the reason why the changes in magnitude of the GMR's of the two systems on annealing are of opposite sign.

Our calculation of the GMR for annealed Fe/Cr samples is based on the same expression, Eq. (1), that we used to calculate the GMR for the annealed Co/Cu samples. The key quantities are again α_b and α_i, the ratios of spin-up electron scattering to spin-down electron scattering in the bulk (b) of the Fe layers and at the Fe/Cr interfaces (i). The Levy-Zhang GMR analysis of spin-dependent interface scattering due to the Friedel resonance shows that a value $\alpha = 12$ accurately reproduces the GMR data for the basic unannealed Fe/Cr system.[54,55] The bulk value of α_b can be obtained by analyzing resistivity data, giving $\alpha_b = 2.7$ according to Darleijn and Miedema,[52] or $\alpha_b = 6$ according to Fert and Campbell.[51] The essential point is that both experimental values yield $\alpha_i > \alpha_b$—a result entirely in accordance with the general assertion[16,37–40] that interface scattering is the major source of spin-dependent scattering for the Fe/Cr system.

This conclusion has important implications for the change of MR on annealing. As already noted in the discussion of Co/Cu, annealing always results in an increase of interface scattering. Consequently, for the Fe/Cr system, annealing will increase the spin-dependent scattering. Inserting the parameters in Eq. (1) shows that this will lead to an initial increase in the magnitude of the MR in accordance with experimental observations.[12,25,31]

In the absence of any detailed information about how annealing affects interfaces in Fe/Cr superlattices, we shall simply assume that the implied changes in the Co/Cu system also applies to Fe/Cr. Thus, for the relatively low annealing temperature of 260 °C, the structural integrity of the sample is maintained and the effect of annealing is to cause interdiffusion of the two atomic species at the interfaces. This is the temperature range in which we predict an increase of the GMR. For superlattices annealed at much higher temperatures, we assume a complete structural breakdown of interfacial integrity. The additional scattering will now be independent of the direction of electron spin, and will lead to a reduction of MR as the superlattices are essentially destroyed. For such temperatures, Eq. (1) predicts that MR should always decrease with annealing for the Fe/Cr system, exactly as we found experimentally for the Co/Cu system. Recent experimental results[30] for high-temperature annealing of Fe/Cr multilayers are in accord with this prediction.

IV. THEORY

Equation (1) was derived by generalizing the "resistor network" model of Edwards, Mathon, and Muniz[42] to include interface electron scattering. Although only bulk electron scattering was considered in their analysis, Edwards, Mathon, and Muniz pointed out that their model can readily accommodate interface electron scattering by adding "resistors" to the network to represent these additional scattering processes. An excellent review of this model has been given by Mathon.[44]

In the measurement of MR, a current flows in the

direction parallel to the layers of the superlattice and the resistance is measured. We consider the case for which the thickness of the nonmagnetic spacer layer produces antiferromagnetic coupling between adjacent magnetic layers. Applying a strong magnetic field then aligns the superlattice ferromagnetically. The electrical resistances of the superlattice in the antiferromagnetic (AFM) and the ferromagnetic (FM) configurations are denoted by R_{AFM} and R_{FM}, respectively, and the normalized magnetoresistance is given by

$$\mathrm{MR}=(R_{\mathrm{AFM}}-R_{\mathrm{FM}})/R_{\mathrm{FM}} \tag{2}$$

The superlattice consists of a series of bilayers (one layer being magnetic and the other layer being nonmagnetic), with the resistance of each bilayer depending on the direction of the electron spin. The higher and the lower resistances of the bilayer for the two different electron spin directions are denoted by H and L. We are considering an electron whose mean free path is long enough that it samples several (at least two) bilayers so that electrons can distinguish between the FM and the AFM configurations. In Fig. 9(a), we depict, for each spin direction, two bilayers in the AFM configuration, and in Fig. 9(b), two bilayers in the FM configuration. The "height" of each layer indicates schematically the magnitude of its resistivity, which depends on spin direction in the magnetic layers (labeled M), but does not in the nonmagnetic layers (labeled N).

In the AFM configuration, electrons of both spin directions experience both the higher and lower resistances H and L, respectively. Therefore, for *both* the spin-up electrons (resistance $R_{\uparrow}$) and the spin-down electrons (resistance $R_{\downarrow}$),

$$\mathrm{AFM}: R_{\uparrow}=R_{\downarrow}=H+L \ . \tag{3}$$

On the other hand, in the FM configuration, the resistance of electrons traversing the double bilayer shown in Fig. 9(b) now depends on the spin direction, so that, in this case,

$$FM: R_{\uparrow}=2H, \quad R_{\downarrow}=2L \ . \tag{4}$$

Since, at the temperatures under consideration here, the degree of spin mixing is small, the spin-up and spin-down electrons constitute two quite separate currents, as if these currents were flowing in separate parallel wires. Therefore, the total resistance of the double bilayer in Fig. 9 is given by adding resistances in parallel. A short calculation then yields a general expression for the MR,

$$\mathrm{MR}=\frac{(H-L)^2}{4HL} \ . \tag{5}$$

The geometrical factors of the length and cross-sectional area of the superlattice are the same in both the AFM and the FM configurations, and so do not appear in (5). Thus, for the calculation of MR, we may equally well view the quantities H and L as the spin-up and the spin-down resistivities of the double bilayers in Fig. 9.

To calculate H and L, we consider separately the contributions due to bulk scattering and due to interface scattering of the electrons. The bulk (b) scattering resistivities, denoted H_b and L_b, are given by the spatial average of the bulk resistivity in the magnetic (m) layers (ρ_m^b) and in the nonmagnetic (n) layers (ρ_n^b). In the magnetic layers, ρ_m^b has a higher value, denoted ρ_{mH}^b, for one spin direction and a lower value, denoted ρ_{mL}^b, for the other spin direction. Taking the spatial average over the bilayers yields

$$\begin{aligned} H_b&=\frac{M\rho_{mH}^b+N\rho_n^b}{M+N} \ , \\ L_b&=\frac{M\rho_{mL}^b+N\rho_n^b}{M+N} \ , \end{aligned} \tag{6}$$

where M and N are the thicknesses of the magnetic and the nonmagnetic layers, respectively.

Now we consider the contribution to the resistivities due to interface electron scattering, which is the new feature of the calculation. The interface resistivty in the double bilayer has a contribution due to electron scattering by nonmagnetic atoms in the magnetic surface layers (denoted ρ_m^i), and one from electron scattering by magnetic atoms in the nonmagnetic surface layer (denoted ρ_n^i). Although the term ρ_n^i is independent of the direction of electron spin, for Fe/Cr superlattices resonant scattering[53] gives ρ_m^i a very strong spin dependence with corresponding high and low interface resistivities denoted by ρ_{mH}^i and ρ_{mL}^i, respectively. The high and low overall interface resistivities for the two spin directions, labeled H_i and L_i, are thus

$$\begin{aligned} H_i&=2\rho_{mH}^i+2\rho_n^i \ , \\ L_i&=2\rho_{mL}^i+2\rho_n^i \ , \end{aligned} \tag{7}$$

where the factor of 2 stems from the two interfaces of the bilayer.

To obtain the total resistivities for the bilayer, H and L, including both bulk and interface electron scattering, one combines (6) and (7) and introduces the important parameters p_b and p_i to denote the relative proportions of bulk and interface electron scattering, respectively, giving

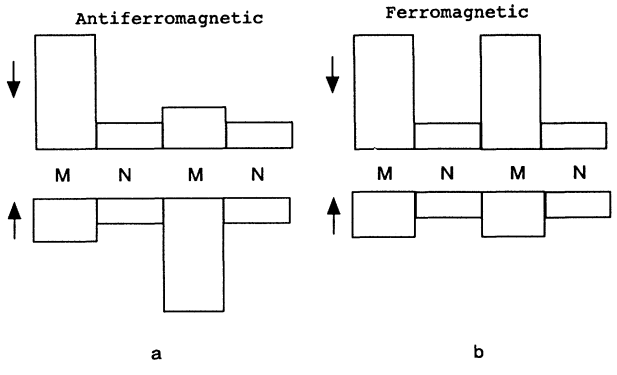

FIG. 9. A schematic diagram illustrating the resistor network model discussed in the text. (a) is the antiferromagnetic configuration and (b) is the ferromagnetic configuration.

$$H = p_b H_b + p_i H_i \ ,$$
$$L = p_b L_b + p_i L_i \ . \tag{8}$$

Inserting (6)–(8) into (5) yields the following expression for MR:

$$\mathrm{MR} = \frac{[\frac{1}{2} M p_b(\rho^b_{mH} - \rho^b_{mL}) + p_i(M+N)(\rho^i_{mH} - \rho^i_{mL})]^2}{D_H D_L} \ . \tag{9}$$

where

$$D_H = p_b(M\rho^b_{mH} + N\rho^b_n) + 2p_i(M+N)(\rho^i_{mH} + \rho^i_n) \ ,$$
$$D_L = p_b(M\rho^b_{mL} + N\rho^b_n) + 2p_i(M+N)(\rho^i_{mL} + \rho^i_n) \ .$$

Although Eq. (9) contains many unknown parameters, we are able to make a number of simplifying assumptions, since we are not attempting to calculate the absolute value of MR, but only its relative change on annealing. This approach is consistent with the results of numerical tests we have made that show that the change in MR on annealing is relatively insensitive to our approximations. The principal guideline to be followed is that the essential "physics" of the change in MR on annealing lies in the spin-dependent parameters.

Our first approximation is to set $\rho^i_n = \rho^b_n$. Since these quantities are both independent of the spin direction, their relative values are unimportant. Our second approximation is to set $\rho^i_n = \rho^i_{mL}$. For the Co/Cu system, ρ^i_m is independent of spin direction, but for the Fe/Cr system, the spin dependence of this magnetic component of the interface layers is central to the whole problem. The entire effect of the Friedel resonance of the virtual bound state is to produce a large enhancement in the value of ρ^i_{mH}, while the value of ρ^i_{mL} is almost unaffected. Our third and final approximation is to set $\rho^b_{mL} = \rho^b_n$. Although the spin dependence of ρ^b_m in the Co/Cu system is very important, the entire effect of the d-band density of states in ferromagnetic Co is to produce a large value for ρ^b_{mH}; the value of ρ^b_{mL} for Co is not influenced by s-d scattering and remains low. Similarly, for the Fe/Cr system, Moruzzi, Janak, and Williams[56] find comparable values for the bulk density of states for Cr and for the spin-down subband of ferromagnetic Fe. This makes our third approximation quite reasonable. Moreover, the ratio of these quantities was found by Edwards, Mathon, and Muniz (who denotes this ratio β) to be close to unity for both the Co/Cu system and the Fe/Cr system. Having made these approximations, it is straightforward to reduce Eq. (9) to the expression for MR given in Eq. (1).

We now turn to the expression for the zero-field resistivity ρ_0. In the absence of a magnetic field, the superlattice is in the AFM configuration, implying from Eqs. (6)–(8) that

$$\rho_0 \propto p_b(M\rho^b_{mH} + M\rho^b_{mL} + 2N\rho^b_n) + 2p_i(M+N)(\rho^i_{mH} + \rho^i_{mL} + \rho^i_n) \ . \tag{10}$$

Invoking our approximations described earlier leads to the final result

$$\rho_0 = \rho_{\mathrm{tot}}[p_b(\alpha_b + 1 + 2r) + 2p_i(1+r)(\alpha_i + 3)] \ , \tag{11}$$

where we denote the constant of proportionality as ρ_{tot} because it represents the total electron scattering expressed in resistivity units. The value of ρ_{tot} for the unannealed superlattice is chosen to make ρ_0 equal to the measured value for that sample (the open circle in Fig. 8), while the value of p_b is taken from the magnetoresistance of the unannealed sample. The effect of annealing is to increase the electron scattering, which increases ρ_{tot} and hence ρ_0.

V. SUMMARY

We have measured the magnetoresistance of a series of MBE-grown Co/Cu superlattices, and have obtained the following results.

(i) For the appropriate thickness of the Cu spacer layer (7–9 Å), we find a GMR of up to 30%, with a saturation magnetic field of over 40 kOe. Antiferromagnetic coupling is indicated by our magnetization curves and by the large magnitude of the saturation field.

(ii) For space layer thicknesses that are either somewhat smaller (5 Å) or somewhat larger (11 Å), the shape of the magnetization curve and the reduced magnitude of the saturation field indicate ferromagnetic coupling, and correspondingly we observe a much smaller magnetoresistance of only a few percent. A second peak in the magnitude of the saturation field was observed at a Cu thickness of about 18 Å, which suggests oscillations in the magnetic behavior with a period of about 10 Å.

(iii) Annealing an antiferromagnetic Co/Cu superlattice leads to a progressive reduction in the magnitude of the GMR. This reduction is found to be gradual at lower annealing temperatures, but becomes much more rapid as the annealing temperatures are increased.

(iv) An empirical calculation has been carried out for the change in the magnetoresistance on annealing the superlattice, which agrees quantitatively with our data for the Co/Cu system.

(v) The calculation is also in accordance with previous data for annealed Fe/Cr superlattices, which exhibit an initial increase in the magnetoresistance upon annealing the Fe/Cr sample at low temperatures. This difference in behavior between the Co/Cu and the Fe/Cr systems is attributed to Friedel resonant scattering at the interfaces of the Fe/Cr superlattice, due to the virtual bound state of Cr atoms in ferromagnetic Fe.

ACKNOWLEDGMENTS

We acknowledge both the Magnetism and Magnetic Materials Initiative of the SERC and the University of Leeds for their strong support of the MBE project. We also acknowledge Peter DeGroot at the University of Southampton for his assistance in the use of the VSM at the University of Southampton.

*Permanent address: Bar-Ilan University, Ramat-Gan, Israel.
[1]P. Grünberg, R. Schreiber, Y. Pang, M. B. Brodsky, and H. Sowers, Phys. Rev. Lett. **57**, 2442 (1986).
[2]C. Carbone and S. F. Alvarado, Phys. Rev. B **36**, 2433 (1987).
[3]M. N. Baibich, J. M. Broto, A. Fert, F. Nguyen Van Dau, F. Petroff, P. Etienne, G. Creuzet, A. Friederich, and J. Chazelas, Phys. Rev. Lett. **61**, 2472 (1988).
[4]C. H. Lee, H. He, F. Lamelas, W. Varva, C. Uher, and R. Clarke, Phys. Rev. Lett. **62**, 653 (1989).
[5]J. J. Krebs, P. Lubitz, A. Chaiken, and G. A. Prinz, Phys. Rev. Lett. **63**, 1645 (1989).
[6]G. Binasch, P. Grünberg, F. Saurenbach, and W. Zinn, Phys. Rev. B **39**, 4828 (1989).
[7]S. S. P. Parkin, N. More, and K. P. Roche, Phys. Rev. Lett. **64**, 2304 (1990).
[8]R. Allenspach, M. Stampanoni, and A. Bischof, Phys. Rev. Lett. **65**, 3344 (1990).
[9]A. Barthelemy, A. Fert, M. N. Baibich, S. Hadjoudj, F. Petroff, P. Etienne, R. Canabel, S. Lequien, F. Nguyen Van Dau, and G. Creuzet, J. Appl. Phys. **67**, 5908 (1990).
[10]S. S. P. Parkin, R. Bhadra, and K. P. Roche, Phys. Rev. Lett. **66**, 2152 (1991).
[11]J. J. de Miguel, A. Cebollada, J. M. Gallego, R. Miranda, C. M. Schneider, P. Schuster, and J. Kirschner, J. Magn. Magn. Mater. **93**, 1 (1991).
[12]F. Petroff, A. Barthelemy, A. Hamzic, A. Fert, P. Etienne, S. Lequien, and G. Creuzet, J. Magn. Magn. Mater. **93**, 95 (1991).
[13]D. H. Mosca, F. Petroff, A. Fert, P. A. Schroeder, W. P. Pratt, Jr., and R. Laloee, J. Magn. Magn. Mater. **94**, L1 (1991).
[14]W. P. Pratt, Jr., S. F. Lee, J. M. Slaughter, R. Loloee, P. A. Schroeder, and J. Bass, Phys. Rev. Lett. **66**, 3060 (1991).
[15]P. Baumgart, B. A. Gurney, D. R. Wilhoit, T. Nguyen, B. Dieny, and V. S. Speriosu, J. Appl. Phys. **69**, 4792 (1991).
[16]B. Dieny, V. S. Speriosu, S. S. P. Parkin, B. A. Gurney, D. R. Wilhoit, and D. Mauri, Phys. Rev. B **43**, 1297 (1991).
[17]F. Petroff, A. Barthelemy, D. H. Mosca, D. K. Lottis, A. Fert, P. A. Schroeder, W. P. Pratt, Jr., R. Loloee, and S. Lequien, Phys. Rev. B **44**, 5355 (1991).
[18]S. S. P. Parkin, Z. G. Li, and D. J. Smith, Appl. Phys. Lett. **58**, 2710 (1991).
[19]P. Grünberg, S. Demokritov, A. Fuss, M. Vohl, and J. A. Wolf, J. Appl. Phys. **69**, 4789 (1991).
[20]J. Unguris, R. J. Celotta, and D. T. Pierce, Phys. Rev. Lett. **67**, 140 (1991).
[21]S. T. Purcell, W. Folkerts, M. T. Johnson, N. W. E. McGee, K. Jager, J. aan de Stegge, W. B. Zeper, and W. Hoving, Phys. Rev. Lett. **67**, 903 (1991).
[22]A. Fuss, S. Demokritov, P. Grünberg, and W. Zinn, J. Magn. Magn. Mater. **103**, L221 (1992).
[23]Y. Obi, K. Takanashi, Y. Mitani, N. Tsuda, and H. Fujimori, J. Magn. Magn. Mater. **104-107**, 1747 (1992).
[24]S. Joo, Y. Obi, K. Takanashi, and H. Fujimori, J. Magn. Magn. Mater. **104-107**, 1753 (1992).
[25]E. E. Fullerton, D. M. Kelly, J. Guimpel, I. K. Schuller, and Y. Brunynseraede, Phys. Rev. Lett. **68**, 859 (1992).
[26]W. F. Egelhoff, Jr. and M. T. Kief, Phys. Rev. B **45**, 7795 (1992).
[27]D. Greig, M. J. Hall, C. Hammond, B. J. Hickey, H. P. Ho, Magn. Magn. Mater. **110**, L239 (1992).
[28]A. E. Berkowitz, J. R. Mitchell, M. J. Carey, A. P. Young, S. Zhang, F. E. Spada, F. T. Parker, A. Hutten, and G. Thomas, Phys. Rev. Lett. **68**, 3745 (1992).
[29]J. Q. Xiao, J. S. Jiang, and C. L. Chien, Phys. Rev. Lett. **68**, 3749 (1992).
[30]Y. Y. Huang, G. P. Felcher, M. Loewenhaupt, and S. S. P. Parkin, Bull Am. Phys. Soc. **37**, 197 (1992).
[31]A. Starr and S. Schultz, Bull. Am. Phys. Soc. **37**, 198 (1992).
[32]M. J. Hall, B. J. Hickey, M. A. Howson, C. Hammond, M. J. Walker, D. G. Wright, D. Grieg, and N. Wiser, J. Phys. Condens. Matter **4**, L495 (1992).
[33]Z. Chun, M. E. Tomlinson, R. J. Pollard, and P. J. Grundy, J. Magn. Magn. Mater. (to be published).
[34]R. J. Highmore, W. C. Shih, R. E. Somekh, and J. E. Evetts, J. Magn. Magn. Mater. **116**, 249 (1992).
[35]R. E. Camley and J. Barnas, Phys. Rev. Lett. **63**, 664 (1989).
[36]J. Barnas, A. Fuss, R. E. Camley, P. Grünberg, and W. Zinn, Phys. Rev. B **42**, 8110 (1990).
[37]P. M. Levy, S. Zhang, and A. Fert, Phys. Rev. Lett. **65**, 1643 (1990).
[38]Y. Wang, P. M. Levy, and J. L. Fry, Phys. Rev. Lett. **65**, 2732 (1990).
[39]S. Zhang and P. M. Levy, Phys. Rev. B **43**, 11 048 (1991); J. Appl. Phys. **69**, 4786 (1991).
[40]P. M. Levy and S. Zhang, J. Magn. Magn. Mater. **93**, 67 (1991).
[41]D. M. Edwards, J. Mathon, R. B. Muniz, and M. S. Phan, Phys. Rev. Lett. **67**, 493 (1991); J. Phys. Condens. Matter **3**, 4941 (1991).
[42]D. M. Edwards, J. Mathon, and R. B. Muniz, IEEE Trans. Magn. **27**, 3548 (1991).
[43]D. M. Edwards and J. Mathon, J. Magn. Magn. Mater. **93**, 85 (1991).
[44]J. Mathon, Contemp. Phys. **32**, 143 (1991).
[45]J. Mathon, J. Magn. Magn. Mater. **100**, 527 (1991).
[46]J. Inoue, A. Oguri, and S. Maekawa, J. Phys. Soc. Jpn. **60**, 376 (1991).
[47]P. Bruno and C. Chappert, Phys. Rev. Lett. **67**, 1602 (1991).
[48]S. S. P. Parkin, Phys. Rev. Lett. **67**, 3598 (1991).
[49]I. A. Campbell and A. Fert, in *Ferromagnetic Materials,* edited by E. P. Wohlfarth (North-Holland, Amsterdam, 1982), Vol. 3, pp. 747–804.
[50]P. Bruno, Phys. Rev. Lett. (to be published).
[51]A. Fert and I. A. Cambell, J. Phys. F **6**, 849 (1976).
[52]J. F. W. Darleijn and A. R. Miedema, J. Phys. F **7**, L23 (1977).
[53]J. Friedel, in *Proceedings of the International School in Physics "Enrico Fermi,"* Course XXXVII, Theory of Magnetism in Transition Metals, edited by W. Marshall (Academic, New York, 1967), pp. 283–318.
[54]The definition of MR used in Ref. 12 differs from the conventional definition given in our Eq. (3). The GMR data reported in Ref. 12 have been converted to conform to our definition of MR.
[55]The value they choose for their parameter $p=0.55$ corresponds to $\alpha_i=12$, according to Eq. (19) of Ref. 40.
[56]V. L. Moruzzi, J. F. Janak, and A. R. Williams, *Calculated Electronic Properties of Metals* (Pergamon, New York, 1978), pp. 76 and 170.

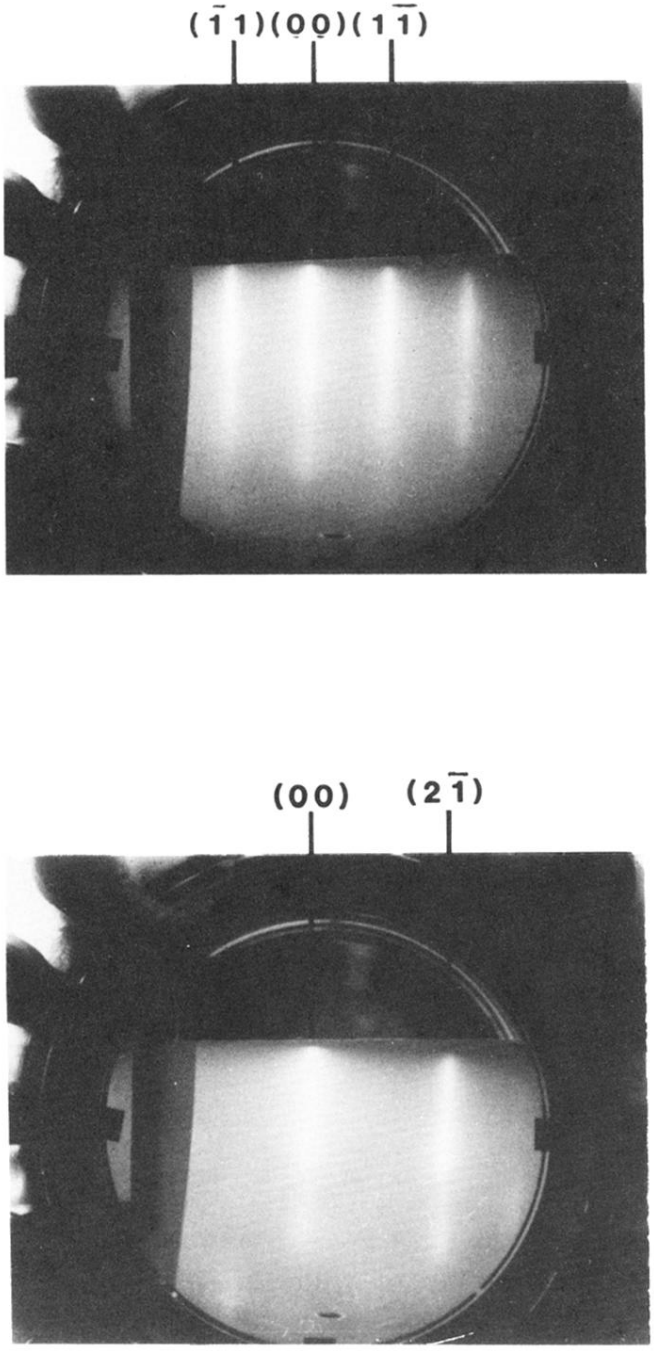

FIG. 1. RHEED patterns on two orientations of the copper surface during growth. The indices refer to the hexagonal net on the (111) surface.